

The Effects of PWM Voltage Source Inverters on the Mechanical Performance of Rolling Bearings

Doyle Busse, Jay Erdman, Russel J. Kerkman, Dave Schlegel, and Gary Skibinski

Allen Bradley Company
6400 W. Enterprise Drive
Mequon, WI 53092
(414) 242 - 8263 FAX (414) 242 - 8300

Abstract - Modern power inverters provide the industrial control industry with significant advantages. The faster switching devices have increased drive performance, but with some recently discovered disadvantages. One disadvantage, rotor shaft voltage and resulting bearing current has become an industry concern. The oil film in a bearing acts as a capacitor and provides a charging mechanism for rotor shaft voltage buildup. Electrical breakdown of the film can damage the bearing. The paper examines the mechanical and electrical characteristics of the bearing and converts them into models. The mechanical model for the bearing contact area establishes an allowable bearing current density, which is used to estimate the effect of electrical life of a mechanical bearing. The electrical model for the bearing provides a significant advancement to aid bearing design and in the analysis of electrically induced bearing damage. Finally, the paper presents quantitative results on one solution to the shaft voltage and bearing current problem.

I. INTRODUCTION

For a drive system control engineer, the interaction of the electrical and mechanical portions of an electrical drive system seldom involves more than the generation of the developed torque and its progression through the drive chain. Recently, however, the effects of power conditioning electronics on mechanical bearings through the mechanism of shaft voltage charging and Electric Discharge Machining (*EDM*) has received considerable exposure [1-4]. Recent investigations show, the Rotor Shaft to Ground Voltage (*V_{rg}*) induced by Pulse Width Modulation (*PWM*) voltage source inverters are quite different in origin from those caused by magnetic dissymmetries reported by Alger in the 1920's [5]. The *V_{rg}* and resulting *EDM* current can cause fluting and failure of the bearing; Fig. 1 shows the consequence of advanced fluting on a bearing race [6].

Through improvements in mechanical design and lubrication, bearing manufacturers, over the last forty years, increased bearing life by optimizing the hydrodynamic characteristics of the bearing. Combining the advances of Adjustable Speed Drives (*ASD*) with the progress in bearing design, however, created a system with unintended

consequences. The hydrodynamic wedge provides a mechanism for *V_{rg}* charging and *EDM* currents, and *dv/dt* induced currents.

For *EDM* to occur, the balls in a bearing must be separated from the race by a dielectric film; the race, film, and balls forming a capacitor. The electrical characteristics of the bearing, therefore, determine the bearing's propensity for fluting. For example, Fig. 2 shows an experimental measurement of the bearing resistance as a function of speed. As motor speed increases, the bearing resistance attains values in the megohm range [1]. This nonconductive bearing characteristic with increasing speed suggests a transition from a resistive element to a more capacitive element as the balls ride the film.

EDM damage, although dramatic, represents only one mechanism for bearing damage from *PWM* and *ASD* operation. Another mechanism occurs with each switching of a power device; the *dv/dt* current through the distributed capacitance. In contrast to *EDM* damage, where actual pieces of molten metal are displaced (Fig. 3) [7], *dv/dt* damage is subtle. The constant barrage of *dv/dt* induces a chemical change in the lubricant, ultimately resulting in a lubricant breakdown. Numerous investigations of the problem have been reported with recent contributions by Costello and Lawson [8,9].

Recently, the authors, in an attempt to quantify, analyze, and reduce *EDM* and *dv/dt* bearing damage, presented their

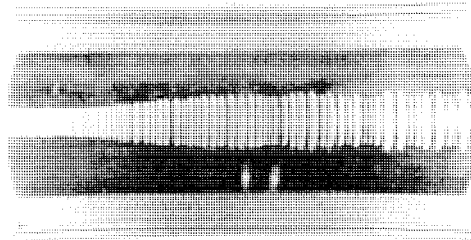


Fig. 1 Surface Roughness of a Ball Bearing Race due to Electrical Fluting [6].

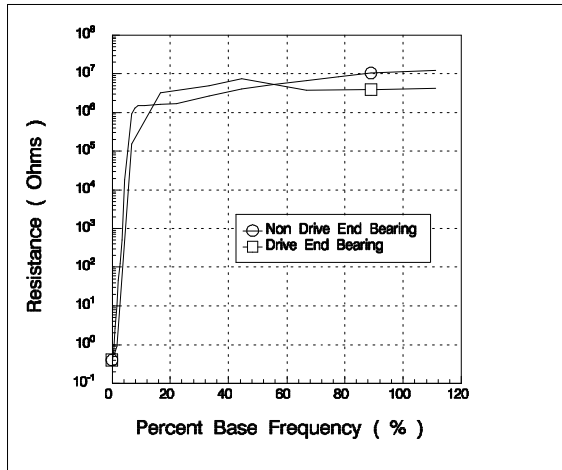


Fig. 2 Bearing Resistance as a Function of Speed.

findings on *PWM* inverter operation and bearing damage [1-3]. The authors propose the Stator to Rotor Capacitance (*C_{sr}*) as the parameter linking *PWM* inverters to *dv/dt* and *EDM* currents. The research culminated with an electrical model of the inverter, motor, and bearing system. The results of that work appear as Fig. 4. Here, the inverter is reduced to its common mode or neutral to ground zero sequence voltage. Cables, common mode chokes, and reactors are represented by the series (*Z_{series}*) and parallel (*Z_{parallel}*) impedances. The motor consists of the common mode equivalent of the stator windings (*L_o* and *r_o*) in series with the important motor capacitances; the Stator to Frame (*C_{sf}*), *C_{sr}*, and Rotor to Frame (*C_{rf}*) Capacitances. The remaining element, the bearing model, is the focus of this paper.

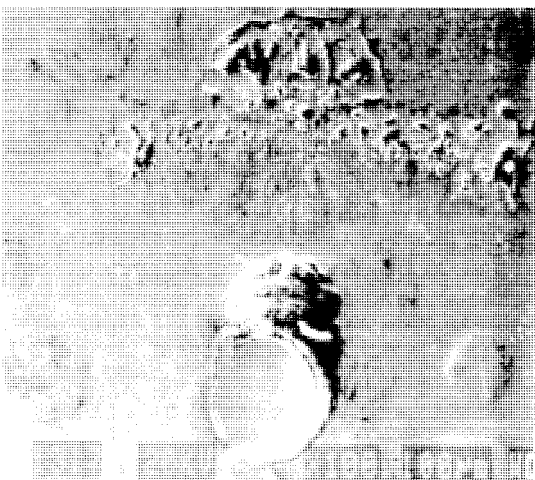


Fig. 3 Microscopic Pits on a Bearing Race due to *EDM* Bearing Current [7].

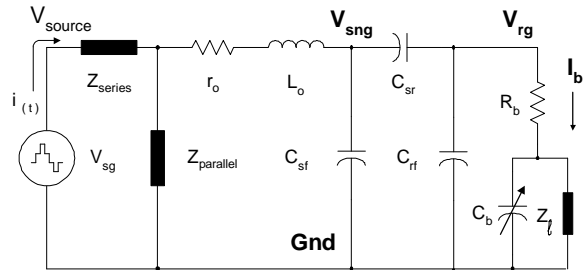


Fig. 4 Common Mode Equivalent Model.

To quantify the effects of *EDM* and *dv/dt* currents on motor bearings, the current density within the bearing is critical [2]. Establishing the current density requires an estimate of the point contact area of the ball - race interface. Section II of the paper presents a procedure for calculating the interface area based on Hertzian point contact theory [10]. With the contact area defined, the effect of other mechanical elements on bearing capacitance determines the extent of *EDM* and *dv/dt* currents. These elements include the load, velocity, and lubricant thickness and condition. The paper continues by incorporating these effects in the Bearing Capacitance (*C_b*) by expanding the bearing model's complexity. The paper concludes with an estimation of the reduced bearing life resulting from *EDM* and *dv/dt* currents with a conventional motor - bearing system and a comparison with an Electrostatic Shielded Induction Motor (*ESIM*), a previously presented solution to the electrostatically induced Bearing Current (*I_b*) problem [1-3].

II. Electrically Induced Bearing Failures and the Hertzian Ellipse Point Contact Area

Bearing failures are attributed to traditional mechanical and thermal failure mechanisms or induced *I_b*. Mechanical failure mechanisms are produced by excessive vibration, while thermal failure results from overloads, which increase bearing temperature and decrease mechanical life. Induced *I_b* results from machine design or application.

Machines contain magnetic dissymmetries inducing end to end sine wave axial *V_{rg}* that results in *I_b*. *I_b* and its induced mechanical wear do not exist if *V_{rg}* is less than a critical bearing Threshold Voltage (*V_{th}*) required to break down the insulating grease [11]. *V_{th}* is 0.2 to 1 volt under 60 Hz sine wave operation [12,13]. This threshold, as pointed out in [2], depends on the form of the excitation and in the case of *PWM ASDs* increases to approximately 30 volts. Low *I_b* is a result of *V_{rg}* being less than *V_{th}*, which induces a chemical change of low resistivity lubricants, ultimately reducing life by raceway corrosion [14]. *V_{rg}* exceeding *V_{th}* can produce damaging *EDM* currents caused by the bearing oil film acting as a capacitor in high resistivity lubricants and charging to open circuit *V_{rg}* levels [1-3]. When race to ball asperity contacts

come close, the oil film electric field increases leading to breakdown with high discharge currents that create a localized elevated temperature of the race and molten pits (Fig. 3). The pits eventually lead to fluting (Fig. 1) and reduced mechanical life [15]. Small machines use inexpensive bearings and therefore ride upon the film less often; thus on average maintaining a V_{rg} less than V_{th} . Large machines or servo motors may employ lubricants with increased V_{th} thus reducing the occurrences of EDM current.

Establishing a maximum allowable I_b magnitude is difficult without knowing surface contact area of the passing current and grease composition. A non-rotating bearing, with its large contact area, may pass large sine wave currents without damage [13]. Also, I_b magnitude failure mechanisms are sensitive to the type of grease. High resistivity mineral oil greases act as capacitors with high V_{th} and produce EDM currents and arcing on discharge. This failure is best analyzed using I_b density. High resistivity greases with low I_b do not produce arcing but may produce fritting. Fritting tempers the steel, which lowers surface hardness. Low resistivity lithium grease does not exhibit a V_{th} but acts as a resistor. Currents of 189 mA rms (267 mA peak) cause grease decomposition into lithium iron oxide, leading to increased wear and bearing failure [14]. Values of 0.5 A rms accelerate corrosion and fritting [14]. Thus, EDM currents and dv/dt currents should be analyzed for allowable I_b density and peak currents < 267 mApk for corrosive effects and fritting.

A. Characteristics of the Bearing Surfaces and Contact Area

Accurate calculation of actual contact surface area in a rotating bearing is difficult, since it depends on surface roughness, "asperity contacts" and the oil film thickness, which itself is a function of grease composition and temperature, motor speed and motor load. Each race and ball surface, viewed at the microscopic level, is composed of a waviness with a surface roughness riding the waviness. This is shown in Fig. 5 [15]. The Hertzian contact area results from the plastic and elastic deformation of two mating surfaces creating an elliptical shaped contact area. Typical Hertzian

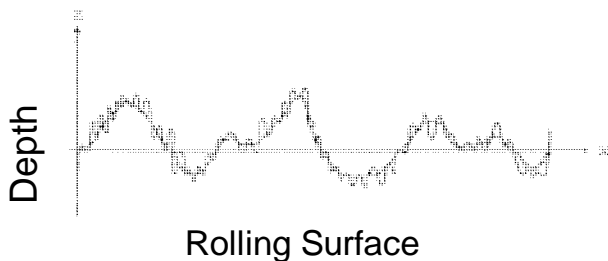


Fig. 5 Bearing Surface Waviness and Roughness [15].

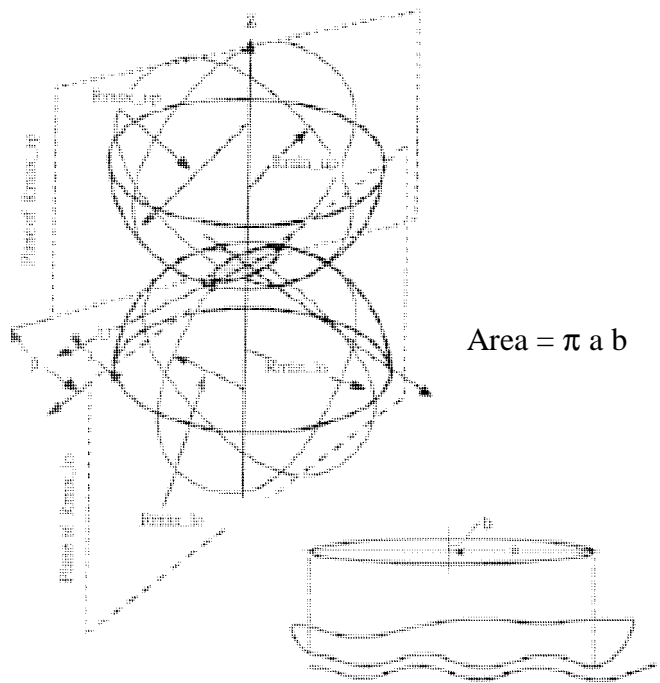


Fig. 6 Hertzian Ellipse Contact Area - Macroscopic and Microscopic Views [10].

contact areas are demonstrated in Fig. 6 through macroscopic and microscopic scaled drawings [10].

B. Calculation of the Asperity Contact Area

Equations based on Hertzian point contact theory as provided by Harris generate curves relating contact area to load [10]. A single row radial ball bearing satisfies the assumptions of the Hertzian equations. The necessary mechanical parameters obtained from bearing manufacturers include: the inner raceway diameter (d_i) in mm, outer diameter (d_o) in mm, ball diameter (D) in mm, two ratios, the inner raceway curvature (r_i_curve) and the outer raceway curvature

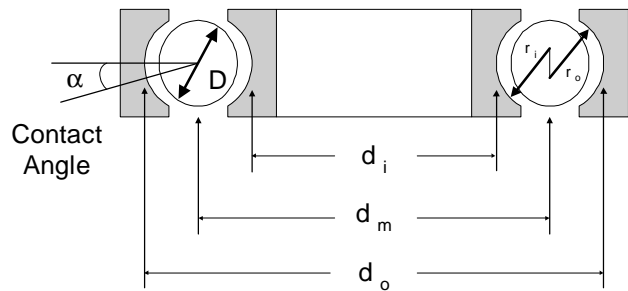


Fig. 7 Dimensions for Bearing Asperity Point Contact Calculations [10].

(*ro_curve*), and the free contact angle (α) in degrees. Fig. 7 identifies some of these mechanical dimensions.

Using the equations from Harris, the contact area can be calculated for the inner and outer bearing race surfaces. First, the point contact area depends on the free contact angle, α , given by (1).

$$\alpha = \cos^{-1} \left(1 - \frac{d_o - d_i - 2D}{2[D(f_i + f_o - 1)]} \right) \quad (1)$$

The contact area also requires the inner and outer groove radii (r_i and r_o), defined by (2).

$$r_i = \frac{ri_curve * D}{2} \quad \text{and} \quad r_o = \frac{ro_curve * D}{2} \quad (2)$$

Next, dimensionless quantities, f_i and f_o , are determined (3).

$$f_i = \frac{r_i}{D} \quad \text{and} \quad f_o = \frac{r_o}{D} \quad (3)$$

As shown in the figure, the pitch diameter is defined as:

$$d_m = \frac{1}{2}(d_i + d_o) \quad (4)$$

The dimensionless quantity γ , which relates ball contact arc length to pitch diameter, is defined by (5).

$$\gamma = \frac{D \cos \alpha}{d_m} \quad (5)$$

The curvature of contacting surfaces is inversely related to the radius. Because the ball and race are in relative motion, inner and outer curvature sums (S_{ri} and S_{ro}) are used and they must reflect the convex or concave surface of the ball and race.

$$\Sigma_{\rho i} = \frac{1}{D} \left(4 - \frac{1}{f_i} + \frac{2\gamma}{1-\gamma} \right) \quad \text{and} \quad \Sigma_{\rho o} = \frac{1}{D} \left(4 - \frac{1}{f_o} + \frac{2\gamma}{1+\gamma} \right) \quad (6)$$

The dimensionless curvature differences for the inner and outer races, $F_{\rho i}$ and $F_{\rho o}$, completes the parameter calculations and are given by (7).

$$F_{(\rho)i} = \frac{\frac{1}{f_i} + \frac{2\gamma}{1-\gamma}}{4 - \frac{1}{f_i} + \frac{2\gamma}{1-\gamma}} \quad \text{and} \quad F_{(\rho)o} = \frac{\frac{1}{f_o} - \frac{2\gamma}{1+\gamma}}{4 - \frac{1}{f_o} - \frac{2\gamma}{1+\gamma}} \quad (7)$$

The inner and outer curvature differences, $F_{\rho i}$ and $F_{\rho o}$, are always between 0 and 1, with 0.9 as a nominal value. Intermediate quantities a^* and b^* , the values of which may be obtained via a table lookup or evaluated with computer methods, relate the curvature difference values to the elliptical areas. These quantities depend on the elliptical eccentricity and the evaluation of complete elliptical integrals of the first and second kind [10]. The intermediate quantities, a^* and b^* , together with the load Q , curvature sums, and a constant

term incorporating the modulus of elasticity, combined through (8) and (9) produce quantities with dimensions of length in mm.

$$a_{in} = 0.0236 a_{in}^* \left(\frac{Q}{\Sigma_{\rho i}} \right)^{\frac{1}{3}} \quad a_{out} = 0.0236 a_{out}^* \left(\frac{Q}{\Sigma_{\rho o}} \right)^{\frac{1}{3}} \quad (8)$$

$$b_{in} = 0.0236 b_{in}^* \left(\frac{Q}{\Sigma_{\rho i}} \right)^{\frac{1}{3}} \quad b_{out} = 0.0236 b_{out}^* \left(\frac{Q}{\Sigma_{\rho o}} \right)^{\frac{1}{3}} \quad (9)$$

Finally, the Hertzian contact area can now be calculated from the major and minor axis. Thus, the inner and outer race-ball ellipse contact areas in mm^2 are given by (10).

$$Area_{in} = a_{in} * b_{in} * \pi \quad Area_{out} = a_{out} * b_{out} * \pi \quad (10)$$

As (8)-(10) show, the contact areas are functions of the load supported by the bearings. Point contact areas were computed for the bearing of the 15 Hp induction machine of [1] as a function of load with a spreadsheet and the results plotted in Fig. 8. Consultation with bearing designers confirmed the reasonableness of the calculations.

III. Mechanical and Lubricant Characteristics and Their Effects on Bearing Capacitance

With the bearing contact area established, this section of the paper will present bearing mechanical variables - load, speed, temperature, and lubricant viscosity and additives - and their effect on the bearing's electrical capacitance. This capacitance, C_b , is the critical mechanical component influencing the magnitude of V_{rg} , EDM and dv/dt currents. First,

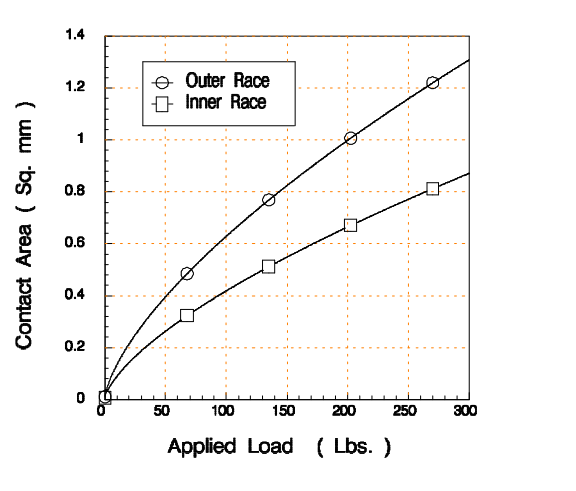


Fig. 8 Bearing Asperity Point Contact as a Function of Applied Load.

operating point parameters - load, speed, temperature, and film thickness - are discussed and their influence on C_b established. This is followed by a review of lubricants and their dielectric characteristics. Finally, this section will close with the development of a new and more detailed model of C_b ; a model incorporating the above mechanical parameters.

A. Operating Point Dependencies

The potential for V_{rg} and I_b depend on the existence of C_b . Furthermore, the bearing impedance becomes capacitive only when a lubricant film occurs in the contact regions between the balls or rollers and the raceways. The minimum film thickness is given by (11).

$$H^0 = 2.65 \bar{U}^{0.7} g^{0.54} / \bar{Q}_z^{0.13} \quad (11)$$

Where U is a function of the fluid velocity and viscosity, g a function of the pressure coefficient of viscosity and modulus of elasticity, and Q the force acting on the ball or roller [10].

Mechanical Load: As discussed in the previous section, bearing contact area establishes the current density at the point of contact between bearing and race. Furthermore, the Hertzian contact size increases with the load raised to 1/n where n depends on the geometries involved [10]. For example, n equals 3 for identical spheres in contact. Thus, with increasing bearing load, the current density through the bearing decreases, reducing the intensity of EDM current. Equation (11) also indicates the film thickness decreases with increasing load, although raised to a very low power ($C_b(Q)$).

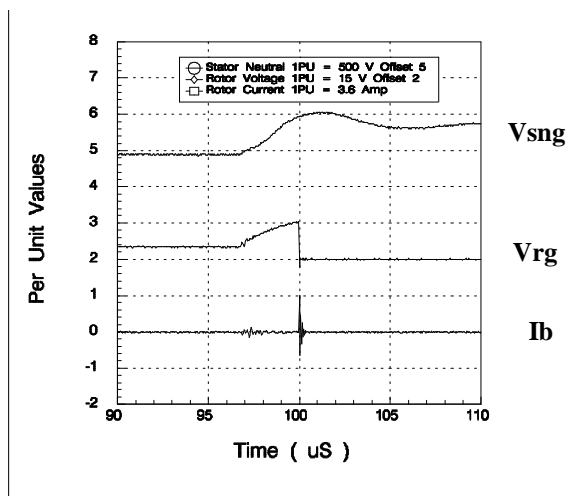


Fig. 9 RC Charging Characteristics of Bearing Shaft Voltage and EDM Discharge Current.

Fig. 9 shows a typical example of the development of V_{rg} . The fact that V_{rg} tracks the Stator Neutral Voltage (V_{sng}) establishes the existence of a film upon which the bearing rides, therefore, developing capacitance C_b . Field measurements, however, indicate a mitigating effect occurs with the addition of a mechanical load. The additional capacitance provided by the mechanical load increases the effective C_b . However, an evaluation of typical laboratory arrangements, wherein a load dynamometer is connected to the ac drive motor, showed V_{rg} was of sufficient magnitude to cause significant EDM current. Generalities about the presence or absence of V_{rg} should therefore be avoided and every application presents a unique capacitive load in parallel with the load motor C_b . Finally, the occurrence of V_{rg} proved independent of torque load; thus, confirming bearing or lateral load determines contact area and not load torque and vibration due to inverter harmonics.

Motor Speed: The existence of V_{rg} depends on the velocity of the lubricant and motor mechanical speed [16]. At low speed, the balls randomly make quasi-contact with the races and prevent V_{rg} buildup. With increasing speed, the balls ride a thin layer of lubricant, the thickness of which is a function of the lubricant's velocity U ($C_b(Q, U)$).

Temperature: The temperature (T) of the bearing depends on the load, speed, mechanical alignment, and lubricant characteristics. The temperature rise due to localized heating from EDM and dv/dt currents creates craters and pits. With the contact time between the ball and outer race larger than the contact time between ball and inner race, bearing wear from EDM and dv/dt currents is greater in the outer race [17]. The lubricant temperature also affects the film thickness; thus C_b is temperature dependent ($C_b(Q, U, T)$).

Lubricant Viscosity: A bearing's capacitance depends on the thickness of the lubricant. However, a lubricant's viscosity (η) determines its flow characteristics and influences C_b . As temperature increases, the viscosity decreases, ultimately reducing the film layer thickness. The viscosity index relates a lubricant's viscosity to its temperature. Furthermore, a lubricant's viscosity partially determines the heat transfer characteristics. An increase in base viscosity will lower the heat transfer coefficient and accelerate oxidation. A decrease in base viscosity reduces oil film thickness and oil circulation, which may accelerate bearing wear. Thus, C_b is a function of the viscosity η ($C_b(Q, U, T, \eta)$).

Lubricant Additives: Commercial lubricants are complex blends, with individual additives chosen for their relative abilities to combat corrosion, friction, wear, load, or other degradation processes. Most bearings are lubricated with grease, which is typically a mineral oil retained within a soap

carrier. Mineral oil is a blend of paraffinic, naphthenic and aromatic petroleum oils. Calcium, sodium, lithium, aluminum complex, and urea based soap carriers are available, each with unique applications. Wang and Tung conducted an investigation on the effects of additives on metal. They discuss a specific case where an oleic acid blended with mineral oil produced a capacitance that is inversely proportional to additive concentration [18]. Thus, C_b is a function of the additive composition λ ($C_b(Q, U, T, \eta, \lambda)$).

C. Oil Film Thickness

In a stationary bearing or bearing rotating at low speed, a large contact area exists between race and ball mainly consisting of quasi-metallic surfaces puncturing through the oil film. These mating surfaces result in the low bearing resistance of Fig. 2 and corresponds to the high friction region of the Stribeck Curve of Fig. 10 [15].

The Stribeck Curve describes *friction vs. (hU/P)*, with h the oil viscosity, U the velocity and P the pressure. Three regimes - boundary film, mixed film, and hydrodynamic film - are shown on the Stribeck Curve. At startup or low sliding speeds within the boundary film region (< 15 rpm) asperity contacts result in high wear and friction. As the speed increases and the bearing enters the mixed film region, the load between the two surfaces is supported partly by the asperities and partly by a lubricating film, resulting in moderate amounts of wear. Finally the bearing enters the hydrodynamic film region (> 90 rpm), the two surfaces are separated by a full lubricant film, resulting in minimal wear [19]. Literature indicates a oil film thickness of 50 \AA to $2 \mu\text{m}$ at normal operating regimes [13,20].

The Stribeck curve, which is inversely related to the *Percent Film vs. Gamma Curve* shown in Fig. 11, demonstrates the mechanical wear relationship of the bearing [1,3]. Fig. 11 converts this to a percent film, which is the amount of time

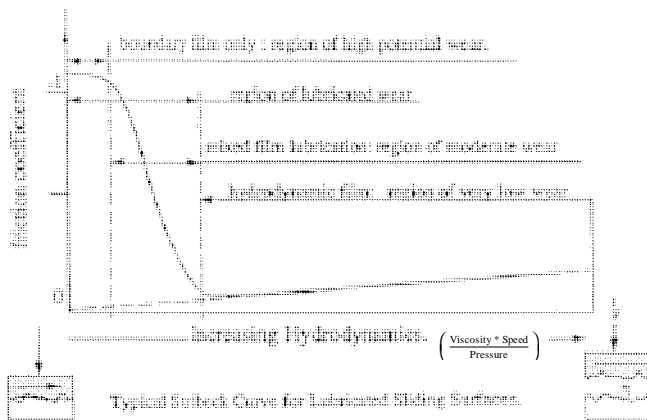


Fig. 10 Stribeck Curve for Lubrication Analysis [15].

the contacting surfaces are fully separated by an oil or lubricating film, while λ (Λ) is the relationship of lubricant film thickness to rms value of contact surface roughness. Thus C_b is a function of the asperity contact area and the lubricant film thickness Λ , ($C_b(Q, U, T, \eta, \lambda, \Lambda)$).

D. Dielectric Properties of Lubricants

Traditionally, dielectric strength is associated with transformer oils and capacitor films. The insulating properties of any material are dependent on its dielectric strength and ability to withstand high voltage without breakdown. The dielectric strength of lubricants as measured by the American Society of Testing and Measurement (ASTM) standard D 877 is a static test with conductive plates 2.5 mm apart. A sinusoidal voltage is applied across the plates and ramped at a rate of 3 kV per second until a leakage current is sensed. Data provided by lubricant vendors indicates a dielectric strength of roughly 15 kV/mm. With high resistance oil and high potentials, a spark can jump across the oil film and cause pitting of the race surface, similar to that caused by EDM in Fig. 3. With low resistance oil and sufficient voltage, corrosion can form on the race surfaces, similar to dv/dt corrosion [21].

Given the typical lubricant film thickness of 0.2 - 2.0 microns, shaft voltages in excess of 2 Vpk under sine wave excitation cause EDM currents [1]. However, as discussed earlier as well as in [1], the pulsed excitation and rate of change of voltage extends the withstand voltage of dielectric materials. Tests reported on in [2] showed a maximum withstand voltage of 30 volts peak at pulse duration's of 10 usecs. Given the typical lubricant film thickness of 0.2 - 2.0 microns, this is equal to a dielectric strength of 15 Vpk/ μm . The debris within the lubricant alters the conductivity and dielectric withstand voltage [19]. As the bearing ages,

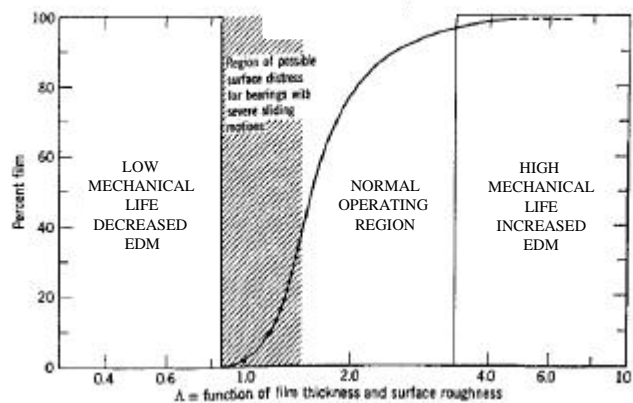


Fig. 11 Percent Film vs. Gamma for a Bearing [10].

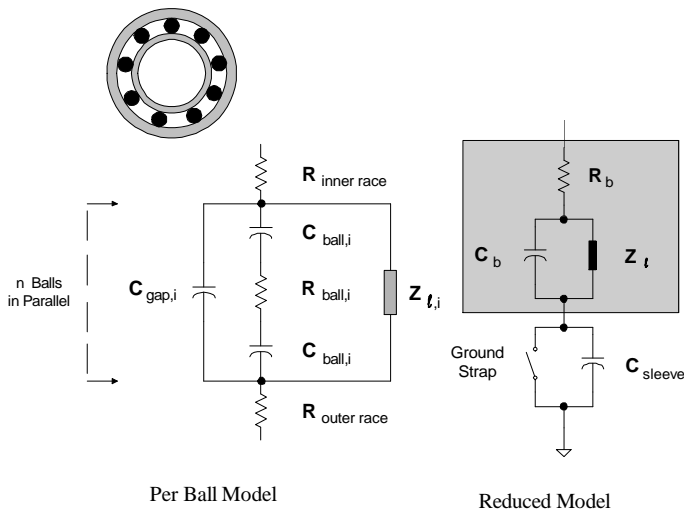


Fig. 12 Motor Bearing Model [1].

mechanical contaminants arising from *EDM* and mechanical wear can significantly alter the lubricants electrical properties. In the extreme, the lubricant becomes a conducting grease, shorting the *C_b* and preventing *V_{rg}* buildup. In fact, one solution to *V_{rg}* buildup and *I_b* is to replace the conventional lubricant with a conductive grease; however, experience with conductive grease indicates the bearing life decreases by a factor of three. Thus *C_b* is a function of the lubricant film's relative dielectric constant ϵ_r ($C_b(Q, U, T, \eta, \lambda, \Lambda, \epsilon_r)$) [16].

E. An Expanded Bearing Model

In a previous paper, the authors proposed a per ball model for a general ball bearing [1]. This model is repeated here as Fig. 12. The model consists of an inner and outer race resistance (*R_{in}* and *R_{out}*) in series with capacitors *C_{ball,i}* representing the film capacitances from outer and inner races to the ball and ball resistance *R_{ball,i}*. These series elements are then in parallel with a capacitance from the outer to inner races and a nonlinear element, which functions to randomly short the bearing outer and inner races replicating the balls penetrating the film layer.

Based on extensive conversations with bearing manufacturers and researchers, and further analysis by the authors, a new per ball electrical model is proposed. This new model incorporates the findings presented above and is presented in Fig. 13. The major differences with the previous model are the division of the lubricant into three regions (outer race oxide, bulk layer, inner race oxide) and the parametric input channels (*Q, U, T, h, I, L, e_r*). The model now incorporates the effects of the mechanical parameters through the nonlinear capacitance and resistance elements. With this model, researchers across a broad range of disciplines have the opportunity of examining the problem of *EDM* and *dv/dt* bearing damage.

IV. Bearing Current Density and Related Life Factors

Bearing failure is best analyzed using *I_b* density. Establishing a maximum allowable *I_b* magnitude can be accomplished by knowing the surface contact area, magnitude of the passing current, and grease composition. Literature indicates a *I_b* density of less than 0.56 Arms/mm² as a safe condition, allowing bearing life of 50,000 hours without electrically influenced damage [2].

The main contributors to electrically based bearing damage are fluting and corrosion. Fluting of the outer race surface is caused by *V_{rg}* charging followed by *EDM* discharge. This occurs when the *V_{rg}* exceeds *V_{ih}* of the oil film, breaking down the film layer. Evidence of *EDM* damage can be seen in Fig. 3, as viewed through a scanning electron microscope. Low resistivity grease does not exhibit a *V_{ih}* but acts as a resistor. Corrosion is caused by an electrochemical reaction between the metal surfaces and the resistivity of the grease. Data presently does not exist for this long term failure mode.

Bearing current testing is historically based on 60 Hz, sine wave, rms amperes with a bearing rotating at rated base speed and using high resistivity grease. Bearing life is therefore based on destructive *EDM* currents occurring due to capacitive discharge breakdowns in high resistivity grease rather than corrosive degradation effects with low resistivity

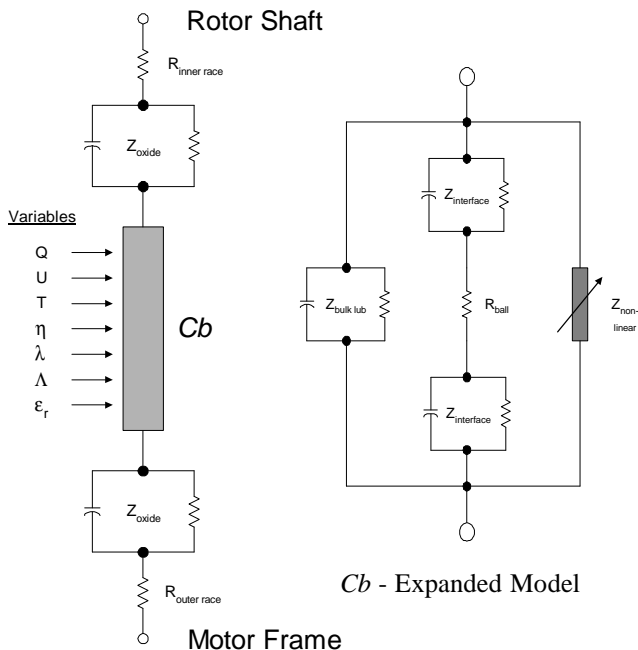


Fig. 13 Improved Bearing Model.

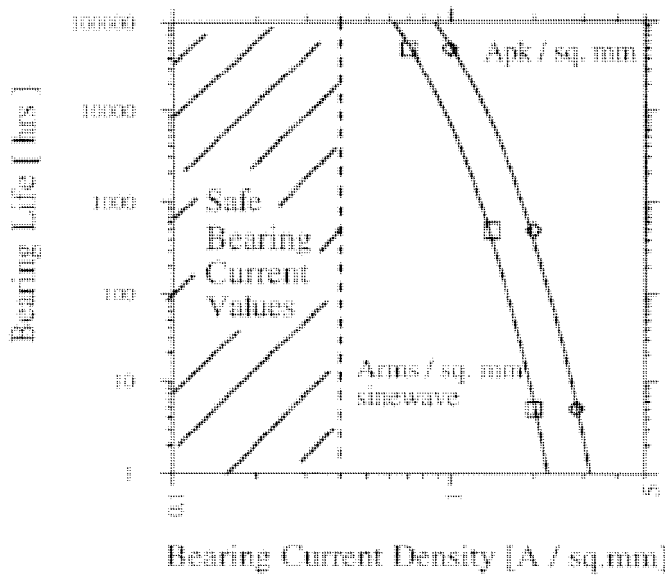


Fig. 14 Bearing Current Density [A / mm²].

greases. The authors convert historical current density (Arms/mm²) to estimate life as shown in Fig. 14 with EDM and *dv/dt Ib* under PWM operation. Equation (12) describes electrical bearing life using data from Fig. 14.

$$Elec\ Life [hrs] = 7,867,204 * 10^{-(2.17[\frac{Apk}{mm^2}])} \quad (12)$$

L₁₀ is the standardized life calculation method for determining mechanical life of a rolling element bearings. It is defined as the number of operating hours at which a bearing can withstand before the first signs of fatigue failure are

apparent. This refers to a statistical nature of which ten percent of the bearings fail in the mode of operation. Typical mechanical life is then defined as five times the L₁₀ life. The basic L₁₀ life calculation is given in (13). In (13), C is the basic dynamic load rating, P is the equivalent dynamic load rating, n is the speed in RPM, and α is the exponent of life equation - a value of three for ball bearings [2,22].

$$Mechanical\ L_{10}\ Life [hrs] = \frac{10^6}{60 n} \left(\frac{C}{P}\right)^\alpha \quad (13)$$

The minimum load on a bearing is also related to ultimate bearing life. Additional factors contributing to failures of properly installed bearings include the duty cycles of the applied load and speed, and the lubrication method, selection, maintenance interval, and contamination. An additional method of determining life of mechanical bearings for ac motors, standardized by the International Standards Organization (ISO), is provided in (14). In (14), a1 is the reliability factor, a2 is the material factor to account for material differences, and a3 is the lubrication factor. The lubrication factor refers to the lubricant film separation of the rolling elements [23].

$$ISO\ Refined\ Life = a1 * a2 * a3 * L_{10}\ life \quad (14)$$

The L₁₀ life establishes a lower limit for bearing life, and for industrial applications is typically 20,000 - 40,000 hours [14], with useful mechanical life approaching 40,000 - 60,000 hours. In comparison, (12) describes bearing life with *Ib* present. Based on this analysis, the author's propose the maximum *Ib* density with PWM drives to be < 0.8 (Apk / mm²) to insure *Ib* does not limit the mechanical life of the bearing.

Table 1. Calculated Bearing Life with PWM IGBT Drives and 15 Hp Motor.

Parameter	Units	Standard AC Motor		ESIM Motor	
		Rotor Weight	3 Times Rotor Weight	Rotor Weight	3 Times Rotor Weight
EDM Current	Apk	2.2	2.2	0	0
Contact Area	mm ²	0.62	1.29	0.62	1.29
Current Density	Apk/mm ²	3.5	1.7	0	0
Calculated Life	hrs	< 10	1,570	> 100,000	> 100,000
dv/dt Current	Apk	0.2 - 0.5	0.2 - 0.5	0.05	0.05
Contact Area	mm ²	0.62	1.29	0.62	1.29
Current Density	Apk/mm ²	0.32 - 0.8	0.15 - 0.38	0.08	0.04
Calculated Life	hrs	> 100,000	> 100,000	> 100,000	> 100,000

V. Bearing Life Projections

Bearing contact area of the test motor bearing (NTN #6208) was calculated as a function of applied load in Fig. 8. Values were extrapolated for applications with no shaft load, so that rotor weight alone is the acting force Q and for applications with shaft force load three times rotor weight. I_b density is determined using measured peak EDM and dv/dt currents and calculated contact area. Estimated bearing life is found using Fig. 14 or (12). The process was repeated with EDM and dv/dt currents measured with the *ESIM* [1-3].

Table 1 shows dv/dt currents do not degrade bearing life. Unloaded motors are more susceptible to EDM I_b damage than loaded motors. The magnitude of calculated bearing life must be tempered by realizing the difficulty of determining contact area and that worst case contact area with one ball bearing was assumed. In real life, the force may be distributed over 1 to 3 ball bearings, increasing contact area, while distributing EDM current pulses. How Fig. 14, the *60 Hz Bearing Current Density vs. Life Curve*, correlates to life with PWM pulsed EDM currents remains unknown. However, EDM I_b densities less than 0.6 to 0.8 Apk/mm² probably do not degrade bearing life. Accurate life predictions are difficult due to the steepness of the life curve, e.g., from 0.8 to 2.0 Apk/mm² life is greatly decreased.

Table 1 shows the *ESIM* proposed in [1-3] appears promising as a solution to I_b problems, since destructive EDM pulse currents are eliminated and dv/dt current is reduced to less than 50 mApk. The problem of low level current causing corrosion and fritting is also eliminated, since dv/dt current is less than 267 mApk. Thus, whether loaded or unloaded, a bearing life of 100,000 hours should be attainable, with mechanical limitations now determining bearing life.

VI. Conclusions

The paper reviewed the mechanical mechanisms contributing to bearing voltage and current. Bearing surface characteristics and failure mechanisms were analyzed. Hertzian Ellipse Theory was employed to calculate bearing point contact area. Relying on established bearing theory and lubricant dielectric strength, the paper recommends I_b densities less than 0.8 Apk/mm², above this value EDM currents are likely. A zero sequence model was reviewed and a bearing model proposed that included mechanical variables affecting the characteristic impedance of the bearing.

The factors contributing to bearing service life were expanded to include electrical and mechanical equations and the ISO related values of reliability, materials and lubricant qualities. The I_b density was used to project the bearing life curve for safe PWM applications.

Data indicates an *ESIM* is capable of reducing I_b to levels less than the maximum recommended value. The dv/dt and

EDM currents produce current densities in line with those observed with sine wave operation. Thus the *ESIM* provides the industry with an attractive solution for damaged bearings resulting from V_{rg} and I_b .

References

- [1] Erdman, Jay, Kerkman, Russel J., Schlegel, Dave, and Skibinski, Gary, "Effect of PWM Inverters on AC Motor Bearing Currents and Shaft Voltages," APEC '95, Tenth Annual Applied Power Electronics Conference and Exposition, March 5-9, 1995, Vol. 1, pp. 24-33.
- [2] Busse, Doyle, Erdman, Jay, Kerkman, Russel J., Schlegel, Dave, and Skibinski, Gary, "Bearing Currents and Their Relationship to PWM Drives," IECON '95, IEEE 21st Annual Industrial Electronics Conference, November 6 - 10, 1995, Vol. 1, pp. 698-705.
- [3] Busse, Doyle, Erdman, Jay, Kerkman, Russel J., Schlegel, Dave, and Skibinski, Gary, "System Electrical Parameters and Their Effects on Bearing Currents," to be presented at APEC '96, Eleventh Annual Applied Power Electronics Conference and Exposition, March 3 - 7, 1996.
- [4] Chen, Shaotang, Lipo, Thomas A., Fitzgerald, Dennis, "Modeling of Motor Bearing Currents in PWM Inverter Drives," IEEE IAS Annual Conference Records, October 8-12, 1995, Vol. 1, pp. 388-393.
- [5] Alger P., Samson H., "Shaft Currents in Electric Machines" A.I.R.E. Conf. Feb. 1924
- [6] Tallian, T., Baile, G., Dalal, H., and Gustafsson, O., "Rolling Bearing Damage - A Morphological Atlas", SKF Industries, Inc., Technology Center, King of Prussia, PA.
- [7] Tallian, T. E., "Failure Atlas for Hertz Contact Machine Elements", ASME Press, New York, 1992
- [8] Costello, M., "Shaft Voltage and Rotating Machinery", IEEE Trans. IAS, March 1993
- [9] Lawson, J., "Motor Bearing Fluting", CH3331-6/93/0000-0032 1993-IEEE
- [10] Harris, T., Rolling Bearing Analysis, Wiley, 3rd edition, 1991
- [11] Kaufman, H., Boyd, J., "The Conduction of Current in Bearings", ASLE Conf, 1958
- [12] NEMA MG-1 Specification Part 31, Section IV, 1993
- [13] Andreason, S. "Passage of Electrical Current thru Rolling Bearings", SKF Gothenburg
- [14] Murray, S., Lewis, P., "Effect of Electrical Currents on Ball Bearing Damage in Vacuum and Air", 22nd ALSE annual meeting May 1, 1967
- [15] Tevaarwerk, J. L. and Glaeser, W. A., "Tribology", University of Wisconsin-Milwaukee, College of Engineering & Applied Science, Center for Continuing Engineering Education, May 15-16, 1995.
- [16] Prashad, H., "Theoretical Evaluation of Capacitance, Capacitive Reactance, Resistance and Their Effects on Performance of Hydrodynamic Journal Bearings," Trans. of the ASME, Oct. 1991, Vol. 113, pp. 762-767.
- [17] Prashad, H., "Theoretical Analysis of the Effects of Instantaneous Charge Leakage on Roller Tracks of Roller Bearings Lubricated with High Resistivity Lubricants Under the Influence of Electric Current," Journal of Tribology, Jan 1990, Vol. 112, pp. 37-43.
- [18] Wang, Simon S., Tung, Simon C., "Using Electrochemical and Spectroscopic Techniques as Probes for Investigating Metal - Lubricant Interactions," STLE Transactions, Vol. 33, pp. 563-572, 1990.
- [19] Tung, Simon C., Wang, Simon S., "Friction Reduction From Electrochemically Deposited Films," STLE Transactions, Vol. 34, pp. 23-34, 1991.
- [20] Prashad, H. "Effect of Operating Parameters on the Threshold Voltages and Impedance Response of Non-Insulated Rolling Element Bearings Under the Action of Electrical Currents," Wear, Vol. 117, 1987, pp. 223-240.
- [21] Godfrey, Douglas, Herguth, William R., "Physical and Chemical Properties of Industrial Mineral Oils Affecting Lubrication," Lubrication Engineering, October, 1995, pp. 825-828.
- [22] Bonnet, A., "Cause and Analysis of Anti-Friction Bearing Failures in AC Induction -Motors", US Electrical Motors Inc.
- [23] Perrin, Martin C., "Large Induction Motor Anti-Friction Bearing Selection," 41st Annual IEEE Petroleum and Chemical Industry Conference, Vancouver, British Columbia, Canada, September, 1994.